This article has been accepted for publication in a future issue of this journal, but has not been fully edited. Content may change prior to final publication. Citation information: DOI 10.1109/JESTPE.2018.2808539, IEEE Journal of Emerging and Selected Topics in Power Electronics

Unified Selective Harmonic Elimination for Cascaded H-bridge Asymmetric Multilevel Inverter

Kehu Yang, *Member, IEEE,* Xinfu Lan, Qi Zhang, and Xin Tang

***Abstract*—The unequal dc-link voltages in the cascaded H-bridge (CHB) asymmetric multilevel inverters lead to asymmetry of the equations for selective harmonic elimination (SHE), which increases the difficulty in solving the switching angles. On the other hand, the unequal dc-link voltages provide a large amount of synthesized waveforms which can be used to optimize the performance of inverters. However, as most of the traditional SHE approaches are derived according to a given output waveform, it cannot handle multiple synthesized waveforms. In this paper, the unified SHE equations are derived for all the possible synthesized waveforms under a specific switching angles distribution among the cells. By using the polynomial homotopy continuation algorithm, all the possible solutions of the unified SHE equations can be found without the selection of initial values. As the waveforms generated by H-bridge are limited to three-level, some of the solutions are not physically realizable and should be discarded, hence, criterion is proposed to distinguish these specious solutions. The case of CHB converter with 2 cells and 6 switching angles are studied, in total, there exist 86 groups of candidate solutions, and 14 of them are physically realizable. Experiments are also shown to validate the correctness of this unified SHE approach for CHB asymmetric multilevel inverters.**

***Index Terms*—Selective harmonic elimination, Multilevel inverter, Cascaded H-bridge, Unequal dc-link voltages, Polynomial homotopy continuation**

I. Introduction

SELECTIVE harmonic elimination (SHE), which has a series of merits, such as low switching losses, low total harmonic distortion (THD), has become one of the popular modulation strategies for multilevel inverters [1]-[9] and has been widely studied during the past several decades [10]. However, most of the existing researches assumed that the dc levels are equal. In the distribution generation system, there are usually several kinds of sources, such as photovoltaic panel, fuel cell, wind turbine, etc., and their output voltages depend heavily on the environment, load or some other factors, which make the dc levels unequal or even time-varying. In some literatures, the multilevel inverters with unequal dc levels are also named asymmetric multilevel inverters (AMLIs) [11],[12]. Although the unequal dc levels lead to asymmetry of the SHE equations, which brings some problems in solving the switching angles. It also provides far more synthesized waveforms than the symmetric muitilevel inverters (SMLIs), which can derive many different SHE equations and probably more valid solutions could be solved and better performance could be achieved. However, first of all, we must explore some new methods which can investigate all the possible synthesized waveforms and identify the optimal one.

Traditionally, the SHE equations are derived according to a given synthesized waveform, and an inequality constraint designates the sequencing of the switching angles, although this way has been widely used in almost all the existing literatures [13]-[18], it still has some defects that can be further improved. For the SMLIs, the amount of synthesized waveforms is equal to the switching patterns (the combination of the transition states on each switching angles), as each switching angle has two possible transition states, the total amount of synthesized waveforms is 2^N, where N is the number of the switching angles. However, for the AMLIs, as the dc levels are unequal, even for the same switching pattern, the synthesized waveforms can be different, so, the overall synthesized waveforms are far more than that of SMLIs. In order to find the optimal switching angles, all the possible synthesized waveforms and all the possible solutions must be evaluated, obviously, these can not be handled by the traditional SHE approaches. Moreover, the inequality constraint limits the algorithms only find solutions within the solution subspace which corresponding to a specific switching pattern, so, the solutions do not satisfy the constraint are considered as "wrong" solutions, but actually, these "wrong" solutions are probably the right solutions for other switching patterns. Recently, a unified SHE approach is proposed [19], in which the various SHE equations for different switching patterns are merged into one group of unified SHE equations and the inequality constraints on the switching angles are also eliminated, however, this approach is limited to the SMLIs. In [20], although this idea is extended to the CHB AMLIs, it is only suitable for fundamental frequency modulation.

On the other hand, the unequal dc levels increase the difficulty in solving the SHE equations. For the numerical iterative methods, the empirical formulas used to compute initial values for the SMLIs are probably unsuitable for the AMLIs. For the intelligent algorithms [21], such as the genetic algorithm (GA) [22], the particle swarm optimization (PSO) [23],[24], the bee algorithm [25], the differential evolution (DE) [26], etc., although the initial values are not necessary, their solving procedures are greatly stochastic and cannot be guaranteed to find correct solutions within a limited time.

Manuscript received August 2, 2017; revised December 18, 2017; accepted February 01, 2018. This work was supported by Beijing Natural Science Foundation (3182031), State Key Laboratory of Alternate Electrical Power System with Renewable EnergySources (LAPS17015), and Fundamental Research Funds for the Central Universities (2009QJ12). Recommended for publication by Associate Editor.

The authors are with the School of Mechanical Electronic and Information Engineering, China University of Mining and Technology, Beijing 100083, China (e-mail: ykh@cumtb.edu.cn).

Color versions of one or more of the figures in this paper are available online at http://ieeexplore.ieee.org.

Digital Object Identifier

2168-6777 (c) 2018 IEEE. Personal use is permitted, but republication/redistribution requires IEEE permission. See http://www.ieee.org/publications_standards/publications/rights/index.html for more information.

This article has been accepted for publication in a future issue of this journal, but has not been fully edited. Content may change prior to final publication. Citation information: DOI 10.1109/JESTPE.2018.2808539, IEEE Journal of Emerging and Selected Topics in Power Electronics

For the algebraic methods, such as the resultant elimination method [27],[28] and the Groebner bases method [29], as their huge computation burden, the symmetric polynomials [30],[31] are usually used to reduce the degrees of the polynomials and then cut down the computation burden. However, as the unequal dc levels in AMLIs, the SHE equations are no longer symmetrical, so, the symmetric polynomials cannot be applied and the computation burden remains extremely high which greatly limits the application of algebraic methods. In recent years, some totally different approaches for SHE have been proposed, such as the four-equation-based method [32],[33], and the artificial neural networks (ANNs) based method [34],[35], as these methods avoid solving the SHE equations, they can be implemented real time, however, these indirect methods are not robust as the direct methods and their accuracy are not guaranteed.

In general, the existing SHE technologies for CHB AMLIs still have some problems need to be improved, in both the mathematical model and the solving algorithm. In this paper, the switching angles are distributed among the CHB converter's cells, and then the unified SHE equations for a given distribution ratio are proposed, which can deal with multiple synthesized waveforms and is suitable for both the fundamental frequency and the high frequency modulation. Also, a polynomial homotopy continuation[37] based method is proposed to solve the unified SHE equations, with its ability to find all the possible solutions, all the possible synthesized waveforms can be evaluated at the same time and the optimal solution can be further identified.

II. Synthesized Waveforms for CHB AMLIs

A. Switching patterns of the H-bridgs in CHB inverters

Fig.1 is the main circuit of a CHB multilevel inverter with 3 cells whose dc sources E_1, E_2 and E_3 are unequal.

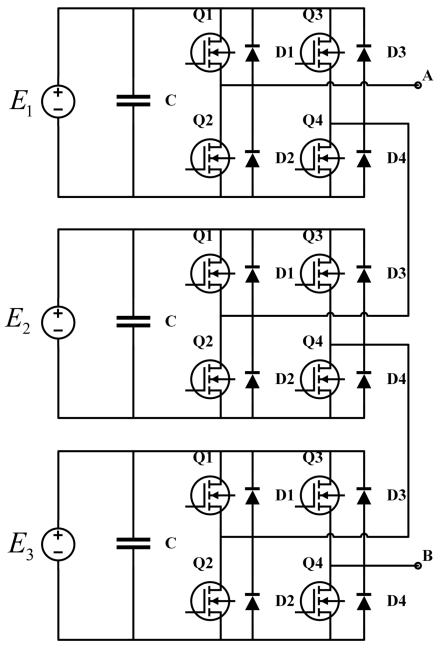

Fig. 1. The main circuit of a CHB multilevel inverter with 3 H-bridges

In the CHB inverter, each cell is a full H-bridge converter which can output three voltage levels E, 0, and $-E$. If there are 3 switching angles in a quarter period, then, the H-bridge has 4 different switching patterns which are shown in Fig.2. For a three-level converter, (a) and (b) are the commonly used switching patterns which are actually identical as they are just out of phase, however, in the CHB inverters, (a) and (b) may lead to different switching patterns. Also, for switching patterns (c) and (d), although they are rarely used in traditional three-level converters, they will introduce new switching patterns in CHB inverters.

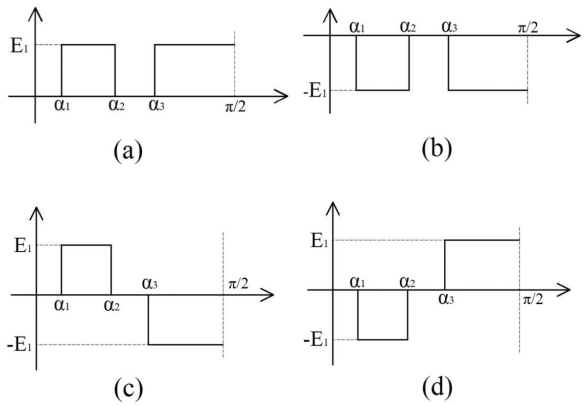

Fig. 2. Switching patterns for 3 switching angles

Generally, if there are n switching angles in a quarter period and the initial voltage level is assumed to 0, the first switching angle has two possible transition states, i.e., the voltage level can both rise to E and fall to $-E$. Then, no matter how the first switching angle goes, the second switching angle has only one transition state that it must be return to level 0. After that, the third switching angle has two transition states again. It can be seen that all the odd number switching angles have two possible transition states whereas all the even number switching angles have only one transition state, so, the total number of the switching patterns of the H-bridges can be computed by the following formula:

$$w(n) = \begin{cases} 2^{n/2} & \text{for } n \text{ is even} \\ 2^{(n+1)/2} & \text{for } n \text{ is odd} \end{cases} \quad (1)$$

Under the traditional SHE framework, different switching patterns result in different SHE equations, hence, for H-bridge with n switching angles, there are w possible SHE equations, which are difficult to be fully studied. However, if the unified ideal proposed in [19] is adopted, all the possible equations can be merged into one unified SHE equations, which can dramatically simplify the solving procedure and provide the opportunity to derive the unified SHE equations for CHB inverters.

B. Distribution ratio and the synthesized waveforms

The output of a CHB inverter is the superposition of the waveforms produced by all its cells. If there are N switching angles, which are assigned to M cells according to a certain

2168-6777 (c) 2018 IEEE. Personal use is permitted, but republication/redistribution requires IEEE permission. See http://www.ieee.org/publications_standards/publications/rights/index.html for more information.

This article has been accepted for publication in a future issue of this journal, but has not been fully edited. Content may change prior to final publication. Citation information: DOI 10.1109/JESTPE.2018.2808539, IEEE Journal of Emerging and Selected Topics in Power Electronics

distribution ratio $\gamma(n_1, n_2, \ldots, n_M)$, the number of the possible switching patterns is

$$W(N, M) = \prod_{i=1}^{M} w(n_i) \tag{2}$$

where $n_1 + n_2 + \cdots + n_M = N$, and $w(n_i)$ can be computed by (1). In CHB AMLIs, although the order of the switching angles in each cell is fixed for a given switching pattern, the order between the cells has many possibilities which can lead to different synthesized waveforms. For example, if each cell in the CHB AMLIs shown in Fig.1 has 3 switching angles, i.e., the distribution ratio is $\gamma(3, 3, 3)$, Fig.3 shows 3 possible synthesized waveforms which are caused by changing the order of switching angles among the cells. Generally, for a given switching pattern, the number of the synthesized waveforms can be computed by the following formula:

$$Z(N, M) = \frac{P(N, N)}{\prod_{i=1}^{M} P(n_i, n_i)} \tag{3}$$

where $P(,)$ is the permutation operation. Hence, the total number of the synthesized waveforms for a given distribution ratio $\gamma(n_1, n_2, \ldots, n_M)$ is the multiplication of $W(N, M)$ and $Z(N, M)$. For distribution ratio $\gamma(3, 3, 3)$, the total number of synthesized waveforms is

$$S[\gamma(3, 3, 3)] = \frac{w(3)w(3)w(3)P(9, 9)}{P(3, 3)P(3, 3)P(3, 3)} = 107520 \tag{4}$$

In the traditional SHE approaches, the SHE equations are derived according to the synthesized waveform which actually indicates the order of all the switching angles, in other words, the switching pattern is fixed. However, even for a simple case that 9 switching angles with distribution ratio $\gamma(3, 3, 3)$, there are 107520 different synthesized waveforms, which will result in 107520 different SHE equations. Among these SHE equations, we don't know which one has solutions or whose solutions have better performance than others. The only way to find the optimal solution is to solve all the 107520 SHE equations, obviously, it is cannot be handled by the traditional SHE approaches.

For the SMLIs, the synthesized waveforms are much less than that of the AMLIs, for example, the number of synthesized waveforms for CHB SMLIs with 9 switching angles is only $2^9 = 512$. The reason for this is that the switching angles in CHB SMLIs are exchangeable among the cells, i.e., the switching angles assigned to a certain cell can also be assigned to other cells, which cannot result in extra synthesized waveforms. However, once the dc levels are unequal, the switching angles are attached to the cells and cannot be exchanged, otherwise, new synthesized waveforms will be produced as the changes on voltage levels lead to different PWM waveforms.

III. Unified SHE Equations for CHB AMLIs

So far, almost all of the existing SHE models for multilevel converters have an inequality constraint on all the switching angles, such as:

$$0 < \alpha_1 < \alpha_2 < \cdots < \alpha_{N-1} < \alpha_N < \frac{\pi}{2}$$

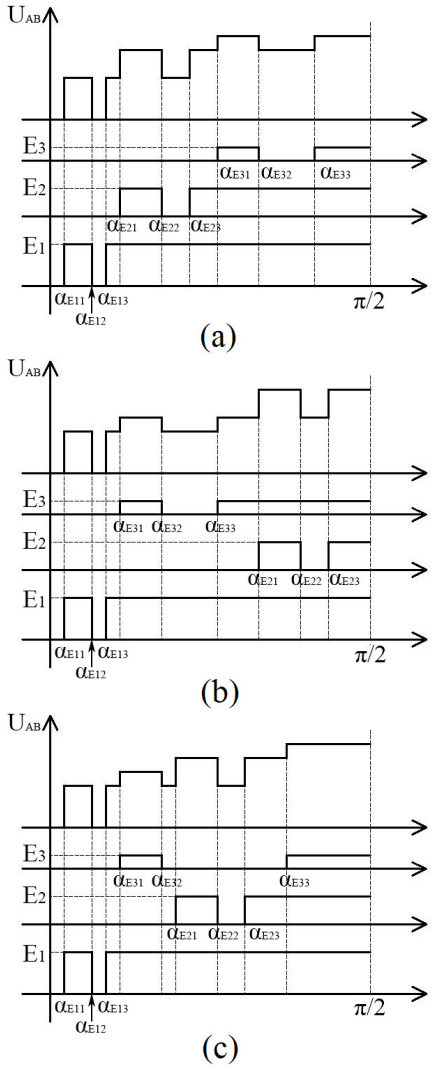

Fig. 3. Synthesized waveforms caused by changing the order of switching angles between the cells

Also, only the solutions which strictly satisfy this constraint are considered as the physically realizable solutions [26]. However, for the CHB multilevel converters, each cell can be controlled independently, hence, only the switching angles which belong to the same cell should have a fixed order. So, it is more reasonable to modify the constraint to the following constraints:

$$\begin{gathered}
0 < \alpha_{11} < \alpha_{12} < \cdots < \alpha_{1n_1-1} < \alpha_{1n_1} < \frac{\pi}{2} \\
0 < \alpha_{21} < \alpha_{22} < \cdots < \alpha_{2n_2-1} < \alpha_{2n_2} < \frac{\pi}{2} \\
\vdots \\
0 < \alpha_{M1} < \alpha_{M2} < \cdots < \alpha_{Mn_M-1} < \alpha_{Mn_M} < \frac{\pi}{2}
\end{gathered}$$

where $\alpha_{i1}, \alpha_{i2}, \ldots, \alpha_{in_i-1}, \alpha_{in_i}$ are the switching angles belong to the ith cell. For CHB SMLIs, these two constraints actually are identical as the switching angles are exchangeable among the cells, however, for CHB AMLIs, the latter constraints are more consistent with the actual behaviors of the CHB inverters and can represent various switching patterns, which extend the search space and increase the possibility to find valid solutions.

2168-6777 (c) 2018 IEEE. Personal use is permitted, but republication/redistribution requires IEEE permission. See http://www.ieee.org/publications_standards/publications/rights/index.html for more information.

This article has been accepted for publication in a future issue of this journal, but has not been fully edited. Content may change prior to final publication. Citation information: DOI 10.1109/JESTPE.2018.2808539, IEEE Journal of Emerging and Selected Topics in Power Electronics

Now, inside each cell, the switching angles still have a constraint and are limited to $[0, \frac{\pi}{2}]$, is it indispensable? No, this constraint actually can be completely removed. For traditional two-level and three-level converters, the rising edge and the falling edge of the output PWM waveform must be strictly interleaved, they never allow two successive rising edges or falling edges, hence, this constraint is reasonable and necessary. However, as discussed in section II-A, the H-bridges in a CHB inverter have many switching patterns, according to the unified ideal proposed in [19], these switching patterns can be formulated by one group of unified SHE equations. Hence, the unified SHE equations for CHB AMLIs can be derived as follows:

$$\begin{cases} \sum_{i=1}^{M}\sum_{j=1}^{n_i} E_i \cos(\alpha_{ij}) = m \cdot \sum_{i=1}^{M} E_i \\ \sum_{i=1}^{M}\sum_{j=1}^{n_i} E_i \cos(k\alpha_{ij}) = 0 \quad k = 3, 5, 7 \cdots \end{cases} \tag{5}$$

where E_i and α_{ij} are the voltage of dc source and the jth switching angle in ith cell, respectively, m is the modulation index which is defined as follows:

$$m = \frac{\pi}{4} \cdot \frac{V}{\sum_{i=1}^{M} E_i} \tag{6}$$

The first equation sets the amplitude of fundamental to a desired value V and the other equations ensure the elimination of some selected harmonics. Unlike the commonly used SHE equations, the prefixed signs of the cosine functions are all plus and the constraint on the switching angles are completely removed in (5), which significantly simplify both the expressions and the solving procedure, and provide a powerful approach to study all the possible switching patterns under a unified framework. One thing should be pointed out is that this unified SHE equations are for a given distribution ratio, for different distribution ratios, different SHE equations should be used.

Generally, the unified SHE equations for multilevel converters assume each switching angle has two possible transition states, i.e., rising or falling. However, as discussed in section II-A, for the H-bridges in the CHB inverters, only the odd number switching angles have two possible transition states whereas all the even number switching angles have only one transition state, hence, among the solutions for (5), there probably exist some solutions that have more than two successive rising edges or falling edges, which are not physically realizable and must be discarded. Let's use s_{ij} to represent the transition state on the jth switching angle in ith cell, and if the transition state is rising, $s_{ij} = 1$, otherwise, $s_{ij} = -1$, then, the combination of transition states belong to ith cell is $\{s_{i1}, s_{i2}, \ldots, s_{in_i}\}$. For example, the combinations of transition states for the waveforms shown in Fig.1 are {1,-1,1}, {-1,1,-1}, {1,-1,-1} and {-1,1,1}, respectively. Once the combination of transition states is obtained, the level number on each switching angle can be computed by the following formula:

$$L_{ij} = \sum_{t=1}^{j} s_{it} \tag{7}$$

Then, the waveform is physically realizable if and only if $|L_{ij}| \leq 1$ hold for any $j \in \{1, 2, \ldots, n_i\}$. If the cells in the cascaded multilevel converter are neutral point clamped (NPC) bridges which can generate five-level waveforms, $|L_{ij}|$ should be no larger than 2 which means that more waveforms are physically realizable.

IV. Solving the Unified SHE Equations with Polynomial Homotopy Continuation Algorithm

As its nonlinear transcendental nature, the SHE equations are difficult to be solved. The commonly used numerical methods and intelligent methods usually require initial values and can only find partial solutions. Although the algebraic methods can find all the solutions without the selection of initial values, the computation burden is extremely huge when the dc levels are unequal as the polynomials are no longer symmetric and cannot be simplified. Compared with the cases of equal levels, the unequal levels result in many more switching patterns which would probably introduce more solutions and provide more choices for SHE in CHB AMLIs. In [36], the polynomial homotopy continuation (PHC) algorithm [37] is firstly introduced to solve the multilevel SHE equations with unequal dc levels and show its capability to find all the solutions without the selection of initial values, however, the solved SHE equations are still under the traditional framework and related to a fixed switching pattern. In this paper, in order to find all the possible switching patterns and the corresponding switching angles, the PHC algorithm is also employed to solve the unified SHE equations.

A. Polynomial Homotopy Continuation Algorithm

The homotopy continuation algorithm is a kind of numerical iterative methods used to solve the nonlinear equation systems, unlike the traditional numerical iterative methods, such as the Newton-Raphson method, this algorithm does not solve the original nonlinear system directly, whereas it constructs a start system whose solutions are easily to find and then approximates the original solutions by using the continuation or path-following methods.

Usually, the homotopy continuation algorithm operates in two main stages. Firstly, the following homotopy mapping equation is constructed:

$$H(\mathbf{x}, \lambda) = c(1-\lambda)G(\mathbf{x}) + \lambda F(\mathbf{x}) = 0 \tag{8}$$

where $G(\mathbf{x}) = H(\mathbf{x}, 0)$ is the start system and $F(\mathbf{x}) = H(\mathbf{x}, 1)$ is the target system which needs to be solved. c is a random complex number and λ is the homotopy parameter. In the second stage, as λ moves from 0 to 1, numerical continuation methods trace the paths that originate at the solutions of the start system towards the solutions of the target system. It can be seen that the homotopy continuation algorithm avoids the selection of initial values which is usually a tough work for the traditional numerical iterative methods. Moreover, it has global convergence property and can find all the numerical solutions in the field of complex numbers.

Obviously, the constructed start system $G(\mathbf{x})$ is critical to the homotopy continuation algorithm, it must satisfy the following three properties:

(1) Triviality. The solutions of start system $G(\mathbf{x})$ are trivial to find.

2168-6777 (c) 2018 IEEE. Personal use is permitted, but republication/redistribution requires IEEE permission. See http://www.ieee.org/publications_standards/publications/rights/index.html for more information.

This article has been accepted for publication in a future issue of this journal, but has not been fully edited. Content may change prior to final publication. Citation information: DOI 10.1109/JESTPE.2018.2808539, IEEE Journal of Emerging and Selected Topics in Power Electronics

(2) Smoothness. No singularities along the solution paths occur, as the continuation parameter λ varies from 0 to 1, we get smooth paths that lead from solutions of $G(\mathbf{x})$ to solutions of $F(\mathbf{x})$.

(3) Accessibility. All isolated solutions can be reached.

In order to find all the solutions of the target system $F(\mathbf{x})$, the solution count of the start system must be not less than the target system. However, the evaluation of solution count for a general nonlinear system is very difficult, but if the target system is pure polynomial system, its solution count can be determined by the polynomial theory, this is the basic idea of the PHC algorithm, which makes it different from the general homotopy continuation algorithms. Considering the following polynomial system:

$$\begin{cases} f_1(x_1, x_2, \ldots, x_n) = 0 \\ f_2(x_1, x_2, \ldots, x_n) = 0 \\ \quad\vdots \\ f_n(x_1, x_2, \ldots, x_n) = 0 \end{cases} \tag{9}$$

Let $F = [f_1, f_2, \ldots, f_n]$ and $\mathbf{x} = [x_1, x_2, \ldots, x_n]$. Denote D is the total degree of the target system $F(\mathbf{x})$ which is defined as follows:

$$D = \prod_{k=1}^{n} \deg(f_k) \tag{10}$$

where $\deg(f_k)$ is the degree of $f_k, k \in [1, 2, \ldots, n]$. According to the famous Bézout's theorem, if $F(\mathbf{x})$ has finite solutions in the complex field, then the count of the isolated solutions is no more than D including the multiple solutions. However, the Bézout's theorem just give an upper bound of the count of the solutions, for many polynomial system, the actual solution count is usually less than D. If a start system is constructed with more solutions than the target system actually have, the extra solution paths may converge to infinite points or multiple solutions which waste a large amount of computing time and memory consumption. Hence, if the upper bound of the solution count for the target system can be exactly evaluated, the computation burden will be reduced dramatically. In [37], some reduction methods are proposed to reduce the target system and give a smaller D. If the reduced degrees of $F(\mathbf{x})$ are $(d_1, d_2, \ldots, d_n)$, the start system can be constructed by the following way:

$$G(\mathbf{x}) = [g_1(x), g_2(x), \ldots, g_n(x)] \tag{11}$$

where $g_k(x) = x_k^{d_k} - c_k$, $k = 1, 2, \ldots, n.$, c_k is a complex number. The PHCpack [38] is a user-friendly software package which contains all the key operations in PHC algorithm, includes the construction of the start system and the homotopy mapping equation, the numerical continuation or path following algorithms, provides us a powerful toolbox to solve the unified SHE equations.

B. Solving the Unified SHE Equations with PHCpack

Let's give an example to illustrate how to solve the unified SHE equations by using PHCpack. The studied case is a CHB converter with 2 cells whose normalized dc voltages are 1 p.u. and 0.6 p.u. respectively, the number of switching angles is 6 and the distribution ratio is $\gamma(4, 2)$, then, according to (5), the unified SHE equations for modulation index $m = 0.8$ are as follows:

$$\begin{cases} \sum_{j=1}^{4} \cos(\alpha_{1j}) + 0.6 \sum_{j=1}^{2} \cos(\alpha_{2j}) = 0.8 \\ \sum_{j=1}^{4} \cos(5\alpha_{1j}) + 0.6 \sum_{j=1}^{2} \cos(5\alpha_{2j}) = 0 \\ \sum_{j=1}^{4} \cos(7\alpha_{1j}) + 0.6 \sum_{j=1}^{2} \cos(7\alpha_{2j}) = 0 \\ \sum_{j=1}^{4} \cos(11\alpha_{1j}) + 0.6 \sum_{j=1}^{2} \cos(11\alpha_{2j}) = 0 \\ \sum_{j=1}^{4} \cos(13\alpha_{1j}) + 0.6 \sum_{j=1}^{2} \cos(13\alpha_{2j}) = 0 \\ \sum_{j=1}^{4} \cos(17\alpha_{1j}) + 0.6 \sum_{j=1}^{2} \cos(17\alpha_{2j}) = 0 \end{cases} \tag{12}$$

As the PHC algorithm can only deal with polynomial systems, (12) must be converted into the following polynomial equations by using the multiple-angle formulas and substituting $\cos(\alpha_{ij})$ with x_{ij}.

$$\begin{cases} x_{11} + x_{12} + x_{13} + x_{14} + 0.6(x_{21} + x_{22}) = 0.8 \\ \sum_{j=1}^{4}(16x_{1j}^5 - 20x_{1j}^3 + 5x_{1j}) + \\ 0.6\sum_{j=1}^{2}(16x_{2j}^5 - 20x_{2j}^3 + 5x_{2j}) = 0 \\ \sum_{j=1}^{4}(64x_{1j}^7 - 112x_{1j}^5 + 56x_{1j}^3 - 7x_{1j}) + \\ 0.6\sum_{j=1}^{2}(64x_{2j}^7 - 112x_{2j}^5 + 56x_{2j}^3 - 7x_{2j}) = 0 \\ \sum_{j=1}^{4}(1024x_{1j}^{11} - \cdots - 11x_{1j}) + \\ 0.6\sum_{j=1}^{2}((1024x_{2j}^{11} - \cdots - 11x_{2j})) = 0 \\ \sum_{j=1}^{4}(4096x_{1j}^{13} - \cdots + 13x_{1j}) + \\ 0.6\sum_{j=1}^{2}(4096x_{2j}^{13} - \cdots + 13x_{2j}) = 0 \\ \sum_{j=1}^{4}(65536x_{1j}^{17} - \cdots + 17x_{1j}) + \\ 0.6\sum_{j=1}^{2}(65536x_{2j}^{17} - \cdots + 17x_{2j}) = 0 \end{cases} \tag{13}$$

Then, (13) are solved by the PHCpack and the multiple solutions are merged into one solution, finally, 86 groups of solutions are obtained in which there inevitably exist some solutions that are not physically realizable by the H-bridges. Table I lists some selected solutions for (13).

TABLE I
SOME SELECTED SOLUTIONS

x_{11}	x_{12}	x_{13}	x_{14}	x_{21}	x_{21}
−0.748	0.481	−0.016	0.767	0.954	−0.426
−0.989	0.623	0.257	0.468	0.768	−0.031
0.918	0.620	0.405	−0.067	−0.800	−0.993

According to the method proposed in [19], the switching angles and the corresponding switching patterns can be recovered by the following way: if $x_{ij} > 0$, $\alpha_{ij} = \cos^{-1}(x_{ij})$ and the transition state is rising, otherwise, $\alpha_{ij} = \pi - \cos^{-1}(x_{ij})$ and the transition state is falling. Then, the switching angles belong to the same cell along with their transition states are rearranged in ascending order according to their values, and the final results are shown in Table II.

TABLE II
SWITCHING ANGLES FOR THE SOLUTIONS IN TABLE I (UNIT: DEGREE)

α_{11}	α_{12}	α_{13}	α_{14}	α_{21}	α_{22}
39.92 ↑	41.55 ↓	61.28 ↑	89.08 ↓	17.43 ↑	64.80 ↓
8.47 ↓	51.50 ↑	62.13 ↑	75.13 ↑	39.84 ↑	88.25 ↓
23.36 ↑	51.72 ↑	66.12 ↑	86.17 ↓	6.97 ↓	36.84 ↓

2168-6777 (c) 2018 IEEE. Personal use is permitted, but republication/redistribution requires IEEE permission. See http://www.ieee.org/publications_standards/publications/rights/index.html for more information.

This article has been accepted for publication in a future issue of this journal, but has not been fully edited. Content may change prior to final publication. Citation information: DOI 10.1109/JESTPE.2018.2808539, IEEE Journal of Emerging and Selected Topics in Power Electronics

The final step is to check whether the waveforms are physically realizable or not. The level numbers on each switching angles are computed according to (7) and listed as follows:

TABLE III
LEVEL NUMBERS ON EACH SWITCHING ANGLES IN TABLE I

L_{11}	L_{12}	L_{13}	L_{14}	L_{21}	L_{22}
1	0	1	0	1	0
-1	0	1	2	1	0
1	2	3	2	-1	-2

It can be seen that except for the first group of switching angles, the level numbers on some switching angles of the other two groups of switching angles are larger than 1, which are marked in red and indicate that the corresponding waveforms are not physically realizable by single H-bridge. However, if the first cell of the CHB converter is a NPC bridge which can generate five-level waveforms, the second group of switching angles are also physically realizable. For the third group of switching angles, the waveforms for the two cells are seven-level and five-level, respectively, which require more complicated converters to realize them.

By using this method, all the 86 groups of switching angles are checked, and there are 14 groups of switching angles can be realized by H-bridges, which are listed in Table IV. One thing should be pointed out is that these 14 groups of solutions are just for one distribution ratio, for this case of 6 switching angles, the possible distribution ratios can be $\gamma(1,5), \gamma(2,4), \gamma(3,3), \gamma(4,2)$ and $\gamma(5,1)$, so, the overall physically realizable solutions are probably far more than 14. In contrast, the maximum solution number for SMLIs with 6 switching angles is just 10. It can be seen that the valid solutions for AMLIs are far more than SMLIs, which provides more choice for harmonic elimination.

TABLE IV
PHYSICALLY REALIZABLE SWITCHING ANGLES (UNIT: DEGREE)

	α_{11}	α_{12}	α_{13}	α_{14}	α_{21}	α_{22}
1	2.74 ↑	8.86 ↓	17.38 ↑	85.65 ↓	65.97 ↓	75.03 ↑
2	19.79 ↑	39.78 ↓	61.64 ↑	86.25 ↓	39.11 ↑	65.62 ↓
3	39.92 ↑	41.55 ↓	61.28 ↑	89.08 ↓	17.43 ↑	64.80 ↓
4	14.87 ↑	50.83 ↓	54.43 ↑	78.02 ↓	23.53 ↑	40.07 ↓
5	7.57 ↑	46.39 ↓	49.71 ↑	56.77 ↓	22.34 ↑	75.02 ↓
6	61.96 ↑	68.07 ↓	74.51 ↑	89.09 ↓	20.18 ↑	79.33 ↓
7	21.17 ↑	65.01 ↓	68.32 ↑	77.29 ↓	7.08 ↑	40.70 ↓
8	22.48 ↑	49.71 ↓	53.79 ↑	80.06 ↓	14.09 ↑	37.27 ↓
9	1.42 ↑	58.44 ↓	79.78 ↑	86.26 ↓	39.82 ↑	65.46 ↓
10	19.80 ↑	41.67 ↓	61.64 ↑	86.26 ↓	42.28 ↑	65.62 ↓
11	18.35 ↑	48.02 ↓	53.31 ↑	75.55 ↓	72.25 ↑	88.94 ↓
12	15.12 ↑	44.94 ↓	62.10 ↑	68.44 ↓	39.89 ↑	88.25 ↓
13	9.86 ↑	63.14 ↓	65.61 ↑	73.86 ↓	22.27 ↑	45.10 ↓
14	2.26 ↑	57.86 ↓	68.54 ↓	75.15 ↑	39.83 ↑	88.25 ↓

Compared with the commonly used numerical and intelligent methods, the biggest benefit of this PHC-based algorithm is its capability to find all the solutions for all possible synthesized waveforms without the selection of any initial values, which is very useful in optimizing the performance of multilevel inverters. The only limitation of this method in practical projects is the computing efficiency, the PHC algorithm follows a huge amount of solution paths, which costs most of the computing time, however, as the solution paths are independent of each other, the paths following operations can be easily distributed on different computing nodes, which provides a potential way to improve the efficiency of the PHC algorithm. In recent years, the Graphic Processing Unit (GPU) based parallel computing has become the most popular and powerful tools in high performance computing and has been widely used in many applications. If the PHC algorithm is parallelized on the most powerful GPUs, such as the Tesla P100 from nVidia [39] which has 3584 computing cores inside, its executing efficiency would gets hundreds of times speedup and finally realize the real time computation of the switching angles.

V. EXPERIMENTAL RESULTS

A single-phase multilevel inverter consists of two cascaded H-bridges as shown in Fig.4 has been built to validate the correctness of switching angles solved by this method, in which the IPM module STGIPS30C60 is used as the switching device and the dc link voltages are set to 100V and 60V, respectively. An ARM Cortex-m4-based microcontroller STM32F407 is used to generate the PWM gating signal and control the multilevel converter, and the load is a 20 Ohm resistor.

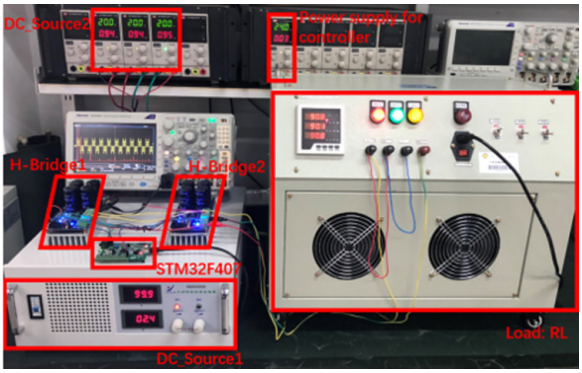

Fig. 4. Experimental set up.

In the experiments, the 4th, 8th, 12th groups of switching angles listed in Table IV are selected to control the CHB inverter. Experimental results including waveforms of the phase voltages and their Fast Fourier Transform (FFT) analysis are shown in Figs.5-7. It can be seen that the aimed 5th, 7th, 11th, 13th and 17th harmonics are eliminated very well, which verifies the correctness of this proposed method.

As shown in Table IV, for one modulation index, there are many groups of solutions, although all of them can precisely eliminate the aimed harmonics, the distributions of the un-eliminated low-order harmonics are different. So, for different applications, we should carefully evaluate the solutions and select the suitable switching angles to control the inverter. Usually, the Total Harmonic Distortion (THD) defined as (14) is used to evaluate the property of the switching angles.

$$\text{THD} = \sqrt{\frac{V_5^2 + V_7^2 + \cdots + V_{49}^2}{V_1^2}} \times 100\% \qquad (14)$$

2168-6777 (c) 2018 IEEE. Personal use is permitted, but republication/redistribution requires IEEE permission. See http://www.ieee.org/publications_standards/publications/rights/index.html for more information.

This article has been accepted for publication in a future issue of this journal, but has not been fully edited. Content may change prior to final publication. Citation information: DOI 10.1109/JESTPE.2018.2808539, IEEE Journal of Emerging and Selected Topics in Power Electronics

However, in some applications, such as common mode voltage mitigation in motor drives and the zero-sequence circulating currents reduction in the paralleling inverter, the zero-sequence harmonics should be limited as low as possible. Here, the Zero-Sequence Harmonic Factor (ZHF) defined as (15) is used to evaluate the quantity of the lowest two zero sequence harmonics, i.e., the 3rd and 9th harmonics.

$$\mathrm{ZHF} = \sqrt{\frac{V_3^2 + V_9^2}{V_1^2}} \times 100\% \tag{15}$$

In addition, the Harmonic Distortion Factor (HDF) which is related to the first two un-eliminated harmonics is another commonly used factor to evaluate the switching angles and it can be calculated by using the following formula:

$$\mathrm{HDF} = \sqrt{\frac{V_{19}^2 + V_{23}^2}{V_1^2}} \times 100\% \tag{16}$$

The experimental and theoretical THD, ZHF and HDF for the 4th, 8th and 12th groups of switching angles are computed and shown in Table V, which shows very good consistency and verifies the correctness of switching angles. It can be seen that the 12th group of switching angles have the lowest zero-sequence harmonics, which are more suitable for common mode voltage mitigation in motor drives. However, their THD and HDF are significant higher than the other two groups of switching angles. From this example, it can be seen that as each group of switching angles have their own harmonic distribution, they should be completely evaluated and carefully selected for different applications to achieve the best performance. Obviously, the unified SHE model and the PHC-based solving method proposed in this paper provide a feasible way to do this.

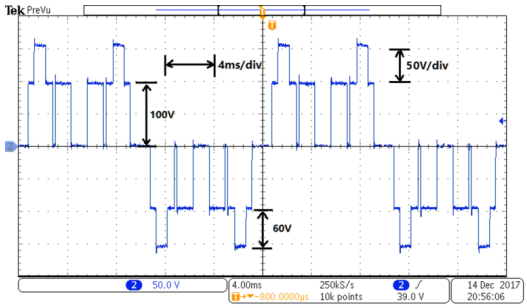

(a) The waveform of the phase voltage.

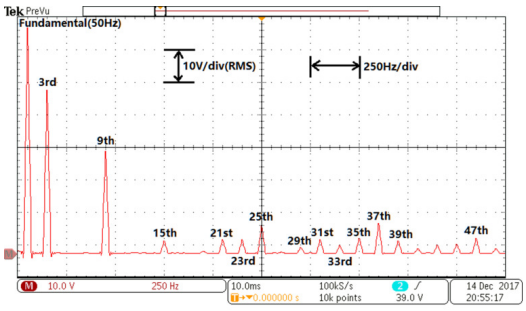

(b) The FFT analysis for the phase voltage in (a).

Fig. 5. Waveform and its FFT for the 4th solution.

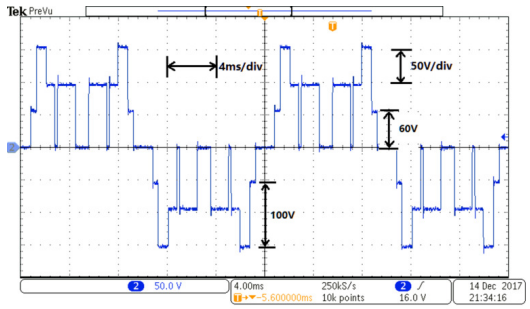

(a) The waveform of the phase voltage.

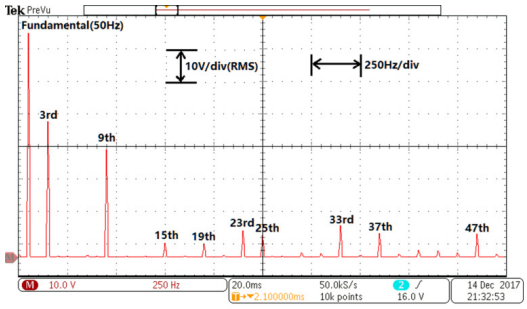

(b) The FFT analysis for the phase voltage in (a).

Fig. 6. Waveform and its FFT for the 8th solution.

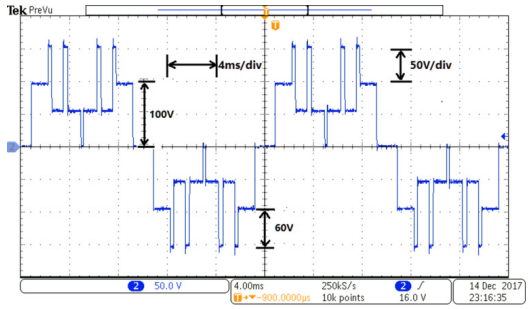

(a) The waveform of the phase voltage.

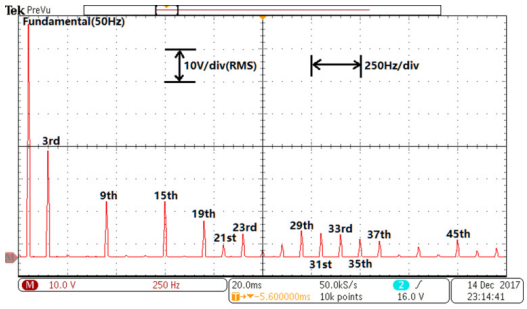

(b) The FFT analysis for the phase voltage in (a).

Fig. 7. Waveform and its FFT for the 12th solution.

TABLE V
THE EXPERIMENTAL AND THEORETICAL THD, ZHF AND HDF

	Experimental Value (%)			Theoretical Value (%)		
	THD	ZHF	HDF	THD	ZHF	HDF
4th	22.73	85.33	5.96	22.88	85.15	6.05
8th	21.95	77.22	12.70	22.28	77.27	12.82
12th	27.72	52.53	18.93	26.72	50.65	18.42

2168-6777 (c) 2018 IEEE. Personal use is permitted, but republication/redistribution requires IEEE permission. See http://www.ieee.org/publications_standards/publications/rights/index.html for more information.

This article has been accepted for publication in a future issue of this journal, but has not been fully edited. Content may change prior to final publication. Citation information: DOI 10.1109/JESTPE.2018.2808539, IEEE Journal of Emerging and Selected Topics in Power Electronics

VI. Conclusion

In this paper, the synthesized waveforms for CHB AMLIs are firstly studied, as the non-commutativity of the switching angles between the H-bridges, the synthesized waveforms produced by AMLIs are much more than SMLIs. Then, a unified selective harmonic elimination approach is proposed, which can simultaneously deal with all the possible synthesized waveforms for a given distribution ratio of switching angles, and the rules used to remove the unrealizable solutions are given. Based on the polynomial homotopy continuation algorithm, a solving instance is given to illustrate how to solve the unified SHE equations. The main advantages of this method are that it has no requirement on initial values and can find all the possible solutions. Experimental results verify the correctness of this unified SHE approach for the CHB AMLIs.

References

[1] Y. Zhang, Y. W. Li, N. R. Zargari, and Z. Cheng, "Improved selective harmonics elimination scheme with online harmonic compensation for high-power PWM converters," *IEEE Trans. Power Electron.*, vol. 30, no. 7, pp. 3508-3517, Jul. 2015.

[2] Y. F. Zhang, D. H. Xu, C. Yan, and S. J. Zou, "Hybrid PWM scheme for the grid inverter," *IEEE J. Emerg. Sel. Topics Power Electron*, vol. 3, no. 4, pp. 1151-1159, Dec. 2015.

[3] H. Zhao, T. Jin, S. Wang, and L. Sun,"A real-time selective harmonic elimination based on a transient-free inner closed-loop control for cascaded multilevel inverters," *IEEE Trans. Power Electron.*, vol. 31, no. 2, pp. 1000-1014, Feb. 2016.

[4] M. Zabaleta, E. Burguete, D. Madariaga, I. Zubimendi, M. Zubiaga, and I. Larrazabal, "LCL grid filter design of a multimegawatt medium-voltage converter for offshore wind turbine using SHEPWM modulation," *IEEE Trans. Power Electron.*, vol. 31, no. 3, pp. 1993-2001, Mar. 2016.

[5] G. Konstantinou, J. Pou, G. J. Capella, K. Song, S. Ceballos, and V. G. Agelidis, "Interleaved operation of three-level neutral point clamped converter legs and reduction of circulating currents under SHE-PWM," *IEEE Trans. Ind. Electron.*, vol. 63, no. 6, pp. 3323-3332, Jun. 2016.

[6] M. Najjar, A. Moeini, M. K. Bakhshizadeh, F. Blaabjerg, and S. Farhangi, "Optimal selective harmonic mitigation technique on variable DC link cascaded H-bridge converter to meet power quality standards," *IEEE J. Emerg. Sel. Topics Power Electron*, vol. 4, no. 3, pp. 1107-1116, Sept. 2016.

[7] M. Sharifzadeh *et al*, "Hybrid SHM-SHE pulse-amplitude modulation for high-power four-leg inverter," *IEEE Trans. Ind. Electron.*, vol. 63, no. 11, pp. 7234-7242, Nov. 2016.

[8] H. Zhao, and S. Wang, "A four-quadrant modulation technique to extend modulation index range for multilevel selective harmonic elimination/compensation using staircase waveforms," *IEEE J. Emerg. Sel. Topics Power Electron*, vol. 5, no. 1, pp. 233-243, Mar. 2017.

[9] C. Buccella, C. Cecati, M. G. Cimoroni, G. Kulothungan, A. Edpuganti, and A. K. Rathore, "A selective harmonic elimination method for five-level converters for distributed generation," *IEEE J. Emerg. Sel. Topics Power Electron*, vol. 5, no. 2, pp. 775-783, Jun. 2017.

[10] M. S. A. Dahidah, G. Konstantinou, and V. G. Agelidis, "A review of multilevel selective harmonic elimination PWM: Formulations, solving algorithms, implementation, and applications," *IEEE Trans. Power Electron.*, vol. 30, no. 8, pp. 4091-4106, Aug. 2015.

[11] E. E. Espinosa, *et al*, "A new modulation method for a 13-Level asymmetric inverter toward minimum THD," *IEEE Trans. Ind. Appl.*, vol. 50, no. 3, pp. 1924-1933, May/Jun. 2014.

[12] E. Samadaei, S. A. Gholamian, A. Sheikholeslami, and J. Adabi, "An envelope type (e-type) module: asymmetric multilevel inverters with reduced components," *IEEE Trans. Ind. Electron.*, vol. 63, no. 11, pp. 7148-7156, Nov. 2016.

[13] S. Sirisukprasert, J. S. Lai, and T. H. Liu, "Optimum harmonic reduction with a wide range of modulation indexes for multilevel converters," *IEEE Trans. Ind. Electron.*, vol. 49, no. 4, pp. 875-881, Aug. 2002.

[14] J. N. Chiasson, L. M. Tolbert, K. J. McKenzie, and Z. Du, "A unified approach to solving the harmonic elimination equations in multilevel converters," *IEEE Trans. Power Electron.*, vol. 19, no. 2, pp. 478-490, Mar. 2004.

[15] M. S. A. Dahidah and V. G. Agelidis, "Selective harmonic elimination PWM control for cascaded multilevel voltage source converters: A generalized formula," *IEEE Trans. Power Electron.*, vol. 23, no. 4, pp. 1620-1630, Jul. 2008.

[16] W. M. Fei, X. B. Ruan, and B. Wu, "A generalized formulation of quarter-wave symmetry SHE-PWM problems for multilevel inverters," *IEEE Trans. Power Electron.*, vol. 24, no. 7, pp. 1758-1766, Jul. 2009.

[17] H. B. Lou, C. X. Mao, D. Wang, J. M. Lu, and L. B. Wang, "Fundamental modulation strategy with selective harmonic elimination for multilevel inverters," *IET Power Electron.*, vol. 7, no. 8, pp. 2173-2181, Aug. 2014.

[18] W. M. Fei, X. B. Ruan, and B. Wu, "A generalized half-wave symmetry SHE-PWM formulation for multilevel voltage inverters," *IEEE Trans. Ind. Electron.*, vol. 57, no. 9, pp. 3030-3038, Sep. 2010.

[19] K. H. Yang *et al*, "Unified selective harmonic elimination for multilevel converters," *IEEE Trans. on Power Electron.*, vol. 32, no. 2, pp. 1579-1590 , Feb. 2017.

[20] K. H. Yang, X. Tang, Q. Zhang, and W. S. Yu, "Unified selective harmonic elimination for fundamental frequency modulated multilevel converter with unequal DC levels," in *Proc. 42nd Annu. Conf. IEEE Ind. Electron. Soc.*, pp. 3623-3628, Florence, Italy, Oct. 24-27, 2016.

[21] A. M. Amjad, and Z. Salam, "A review of soft computing methods for harmonics elimination PWM for inverters in renewable energy conversion systems," *Renewable and Sustainable Energy Reviews*, vol. 33, pp. 141-153, May. 2014.

[22] S. S. Lee, B. Chu, N. R. N. Idris, H. H. Goh, and Y. E. Heng, "Switched-battery boost-multilevel inverter with GA optimized SHEPWM for standalone application," *IEEE Trans. Ind. Electron.*, vol. 63, no. 4, pp. 2133-2142, Apr. 2016.

[23] H. Taghizadeh, and M. T. Hagh, "Harmonic elimination of cascade multilevel inverters with nonequal DC sources using particle swarm optimization," *IEEE Trans. Ind. Electron.*, vol. 57, no. 11: 3678-3684, Nov. 2010.

[24] K. Shen *et al*, "Elimination of harmonics in a modular multilevel converter using particle swarm optimization-based staircase modulation strategy," *IEEE Trans. Ind. Electron.*, vol. 61, no. 10, pp. 5311-5322, Oct. 2014.

[25] A. Kavousi, B. Vahidi, R. Salehi, M. Bakhshizadeh, N. Farokhnia, and S. S. Fathi, "Application of the bee algorithm for selective harmonic elimination strategy in multilevel inverters," *IEEE Trans. Power Electron.*, vol. 27, no. 4: 1689-1696, Apr. 2012.

[26] A. M. Amjad, Z. Salam, and A. M. A. Saif, "Application of differential evolution for cascaded multilevel VSI with harmonics elimination PWM switching," *International Journal of Electrical Power and Energy Systems*, vol. 64, pp. 447-456, Jan. 2015.

[27] J. N. Chiasson, L. M. Tolbert, K. J. McKenzie, and Z. Du, "A complete solution to the harmonic elimination problem," *IEEE Trans. Power Electron.*, vol. 19, no. 2: 491-499, Mar. 2004.

[28] K. H. Yang, L. Y. Chen, J. J. Zhang, J. Hao, and W. S. Yu, "Parallel resultant elimination algorithm to solve the selective harmonic elimination problem," *IET Power Electron.*, vol. 9, no.1, pp. 71-80, Jan. 2016.

[29] K. H. Yang, Z. B. Yuan, R. Y. Yuan, W. S. Yu, J. X. Yuan, and J. Wang, "A Groebner bases theory-based method for selective harmonic elimination," *IEEE Trans. on Power Electron.*, vol. 30, no. 12: 6581-6592, Dec. 2015.

[30] J. N. Chiasson, L. M. Tolbert, K. J. McKenzie, and Z. Du, "Elimination of harmonics in a multilevel converter using the theory of symmetric polynomials and resultants," *IEEE Trans. Contr. Syst. Technol.*, vol. 13, no. 2: 216-223, Mar 2005.

[31] K. H. Yang, Q. Zhang, R. Y. Yuan, W. S. Yu, J. X. Yuan, and J. Wang, "Selective harmonic elimination with Groebner bases and symmetric polynomials," *IEEE Trans. on Power Electron.*, vol. 31, no. 4: 2742-2752 , Apr. 2016.

[32] J. Wang, and D. Ahmadi, "A precise and practical harmonic elimination method for multilevel inverters," *IEEE Trans. Ind. Appl.*, vol. 46, no. 2: 857-865, Mar/Apr. 2010.

[33] D. Ahmadi, K. Zou, C. Li, Y. Huang, and J. Wang, "A universal selective harmonic elimination method for high-power inverters" *IEEE Trans. Power Electron.*, vol. 26, no. 10: 2743-2752, Oct. 2011.

[34] F. Filho, H. Z. Maia, T. H. A. Mateus, B. Ozpineci, L. M. Tolbert, and J. O. P. Pinto, "Adaptive selective harmonic minimization based on ANNs

2168-6777 (c) 2018 IEEE. Personal use is permitted, but republication/redistribution requires IEEE permission. See http://www.ieee.org/publications_standards/publications/rights/index.html for more information.

This article has been accepted for publication in a future issue of this journal, but has not been fully edited. Content may change prior to final publication. Citation information: DOI 10.1109/JESTPE.2018.2808539, IEEE Journal of Emerging and Selected Topics in Power Electronics

for cascade multilevel inverters with varying DC sources," *IEEE Trans. Ind. Electron.*, vol. 60, no. 5, pp. 1955-1962, May. 2013.

[35] M. Balasubramonian, and V. Rajamani, "Design and real-time implementation of SHEPWM in single-phase inverter using generalized hopfield neural network," *IEEE Trans. Ind. Electron.*, vol. 61, no. 11, pp. 6327-6336, Nov. 2014.

[36] K. H. Yang, D. Y. Lu, X. Q. Kuang, Z. B. Yuan, and W. S. Yu,"Harmonic elimination for multilevel converters with unequal DC levels by using the polynomial homotopy continuation algorithm," in *Proc. 35th Chinese Control Conference.*, pp. 9969-9973, Chengdu, China, Jul. 27-29, 2016.

[37] J. Verschelde, Homotopy Continuation Methods for Solving Polynomial Systems, Ph.D. dissertation, University of Leuven, 1996.

[38] J. Verschelde, "PHCpack: A general-purpose solver for polynomial systems by homotopy continuation," *ACM Transactions on Mathematical Software*, vol. 25, no. 2, pp. 251-276, 1999.

[39] Nvidia.com, "NVIDIA Tesla P100, Infinite Compute Power for the Modern Data Center", 2015. [Online]. Available: http://www.nvidia.com/object/tesla-p100.html. [Accessed: 13-Dec-2015].

Kehu Yang (M'13) received the B.S. degree in electrical engineering from the Northwestern Polytechnical University, Xi'an, China, in 2003, and the Ph.D. degree in control theory and control engineering from the Institute of Automation, Chinese Academy of Sciences, Beijing, China, in 2009.

He is currently a Professor at the China University of Mining and Technology, Beijing. From Nov. 2013 to Nov. 2014, he was a Postdoctoral Research Fellow at the Department of Electrical and Computer Engineering, The Ohio State University, Columbus, OH, USA, working on selective harmonic elimination technology and its applications in high-power converter and electric drives. His research interests include harmonic control technologies, modeling and control methods for high-power converters and the applications of computer algebra in power electronics.

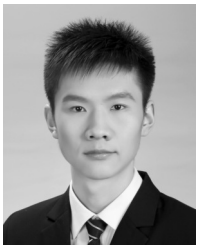

Xinfu Lan was born in Fuyang, Anhui Province, China, on December 20, 1992, he received the B.S. degree in electrical engineering from the China University of Mining and Technology, Beijing, China, in 2016, where he is currently working toward the M.S. degree in the area of power electronics. His current research interests include harmonic control technologies and multilevel converter.

Qi Zhang was born in Puyang, Henan province, China, on July 05, 1991, he received the B.S. degree in electrical engineering from the China University of Mining and Technology, Beijing, China, in 2015, where he is currently pursuing the M.S. degree in the area of power electronics. His current research interests include harmonic control technologies and multilevel converter.

Xin Tang was born in Baoji, Shanxi province, China, on April 27, 1992, she received the B.S. degree in electrical engineering and the M.S. degree in power electronics both from the China University of Mining and Technology, Beijing, in 2014 and 2017, respectively. She is currently working in the field of variable frequency converter in Vertiv Tech Co. Ltd.

2168-6777 (c) 2018 IEEE. Personal use is permitted, but republication/redistribution requires IEEE permission. See http://www.ieee.org/publications_standards/publications/rights/index.html for more information.